J Electroceram (2010) 24:83–90
DOI 10.1007/s10832-008-9456-8

Na^+-fast ionic conducting glass-ceramics of silicophosphates

Toshinori Okura · Hideki Monma · Kimihiro Yamashita

Received: 22 November 2007 / Accepted: 13 February 2008 / Published online: 6 March 2008

Abstract The Na^+-fast ionic conducting glass-ceramics with $Na_5YSi_4O_{12}$ (N5)-type structure were successfully synthesized using the composition formula of $Na_{3+3x-y}R_{1-x}P_ySi_{3-y}O_9$ for a variety of rare earth ions, *R*, under the appropriate composition parameters. In the crystallization of N5-type glass-ceramics, its relatives ($Na_3YSi_3O_9$ (N3)- and $Na_9YSi_6O_{18}$ (N9)-type glass-ceramics) structurally belonging to the family of $Na_{24-3x}Y_xSi_{12}O_{36}$ were found to crystallize as the precursor phase at low temperatures. In order to produce N5 single phase glass-ceramics, the concentration of both phosphorus and rare earth was found important. The meaning of the composition was evaluated by thermodynamic and kinetic studies on the phase transformation of metastable N3 or N9 phases to stable N5 phase with Na^+-fast ionic conductivity. The possible combinations of *x* and *y* became more limited for the crystallization of the fast ionic conducting phase as the ionic radius of *R* increased, while the Na^+ conduction properties were more enhanced in the glass-ceramics of larger *R*. These results are discussed in view of the structure and the conduction mechanism. Also studied were the microstructural effects on the conduction properties, which were dependent upon the heating conditions of crystallization. These effects were understood in relation to the grain boundary conduction properties as well as the transmission electron microstructural morphology of grain boundaries.

Keywords Glass-ceramics · Silicophosphate · Crystallization · Microstructure · Conduction properties

T. Okura (✉) · H. Monma
Department of Materials Science and Technology,
Faculty of Engineering, Kogakuin University,
2665-1 Nakano,
Hachioji, Tokyo 192-0015, Japan
e-mail: okura@cc.kogakuin.ac.jp

H. Monma
e-mail: monma@cc.kogakuin.ac.jp

K. Yamashita (✉)
Institute of Biomaterials and Bioengineering,
Tokyo Medical and Dental University,
2-3-10 Kanda-Surugadai,
Chiyoda, Tokyo 101-0062, Japan
e-mail: yama-k.bcr@tmd.ac.jp

1 Introduction

The use of glass-making processing is favorable for the fabrication of Na^+ conducting electrolyte tubes, which has been the key to the technological development of 1 MW Na/S secondary battery plants. However, the processing technique cannot be applied to well-known β- and β″-aluminas (e.g., $NaAl_{11}O_{17}$ and $NaAl_5O_8$) and Nasicons ($Na_{1+x}Zr_2P_{3-x}Si_xO_{12}$) because their high inclusion of Al_2O_3 or ZrO_2 brings about the inhomogeneous melting or crystallization from glasses. Alternatively, Nasicon-like glass-ceramics were synthesized using the composition with lower content of ZrO_2 ($mNa_2O{\cdot}xZrO_2{\cdot}yP_2O_5{\cdot}(100\text{-}m\text{-}x\text{-}y)SiO_2$ [m=20, 30 mol%]), however, the conductivities (σ) attained were, at most, as high as $\sigma_{300}=2\times10^{-2}$ S/cm at 300 °C with the activation energies (E_a) of approximately 30 kJ/mol [1]. These low conductivities were attributed to the crystallization of the poorly conductive rhombohedral phase in these Nasicon-like materials [1]. $Na_5YSi_4O_{12}$ (N5), which comprises 12-$(SiO_4)^{4-}$-tetrahedra membered skeleton structure (Fig. 1) [2, 3], is another Na^+-fast ionic conductor with $\sigma_{300}=1\times10^{-1}$ S/cm and E_a=25 kJ/mol [4–6]. A pioneering work on N5-type glass-ceramics has been performed by Banks et al. on the family of N5-type materials by substituting Y with Er, Gd or Sm [7].

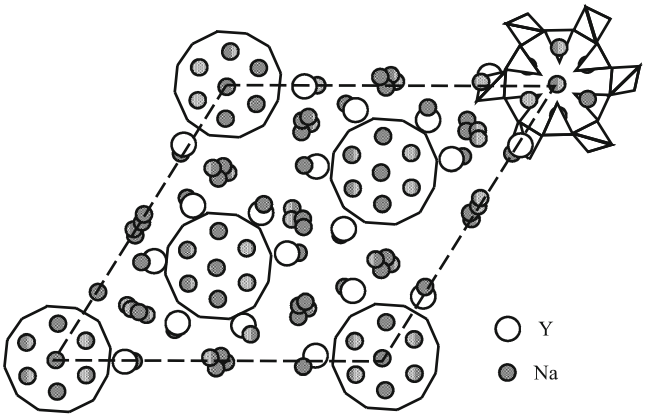

Fig. 1 Crystal structure of $Na_5YSi_4O_{12}$

However, their results were not completely satisfactory because of the relatively lower conductivities of $\sigma_{300}<2\times10^{-2}$ S/cm than the reported values of N5 [7]. This discrepancy may possibly have arisen from the occurrence of a less conductive metastable phase during crystallization [8], as is discussed below.

Contrary to the results of Banks et al., the present authors have produced glass-ceramics with $\sigma_{300}=1\times10^{-1}$ S/cm and $E_a=20$ kJ/mol [9], which were based on the phosphorus-containing N5-type materials discovered in the Na_2O–Y_2O_3–P_2O_5–SiO_2 system [9]. These N5-type materials have been obtained, as well as $Na_3YSi_3O_9$ (N3)-type [10–12] materials, with the composition formula originally derived for N3-type solid solutions and expressed as follows [13],

$$Na_{3+3x-y}Y_{1-x}P_ySi_{3-y}O_9 (x< 0.6, y< 0.5) \quad (1)$$

With the aim of searching for more conductive glass-ceramic N5-type materials, the verification of the validity of the generalized composition formula

$$Na_{3+3x-y}R_{1-x}P_ySi_{3-y}O_9 \quad (2)$$

for the synthesis of other kinds of rare earth N5-type glass-ceramics was studied first. Formula 2 is rewritten with formula 3 according to the formula N5.

$$Na_{4(3+3x-y)/3}Y_{4(1-x)/3}P_{4y/3}Si_{4(3-y)/3}O_{12} \quad (3)$$

In relation to previous works [9, 13], formula 2 was employed in this work, and formula 3 is referred to in the results. The trivalent ions employed here for R^{3+} were Sc^{3+}, In^{3+}, Er^{3+}, Gd^{3+}, Sm^{3+}, Eu^{3+}, Nd^{3+} and La^{3+} as well as Y^{3+}. These results are to be interpreted in terms of the effect of the rare earth ions on the crystallization of N5-type phase in glasses [14–19].

In the course of the fundamental studies on glass-ceramic $Na_{3+3x-y}R_{1-x}P_ySi_{3-y}O_9$, we have interestingly found the crystallization of those N3- and $Na_9YSi_6O_{18}$ (N9)-type phases as the precursors in the glasses [20]. These are the analogues to the silicates N3 and N9 [9, 21] and therefore are the same members of the family of $Na_{24-3x}Y_xSi_{12}O_{36}$ [11] as N5. Although we had also successfully synthesized those materials by the solid-state reactions of powders with the above composition of various sets of the parameters x and y [9, 21], the metastability of those precursor phases had not been noticed in the synthesis. It has been observed that such precursor phases were transformed to the Na^+-fast ionic conducting phase on specimens with appropriate sets of x and y. The present paper will deal with the thermodynamic and kinetic study on the phase transformation of metastable phases to the stable phase with Na^+-fast ionic conductivity. The superiority of our present materials to the other silicate N5 will also be detailed based on the kinetic results.

The microstructure of a glass-ceramic, including neck growth among grains as well as grain size, is generally affected by the crystallization process [22]. As the above mentioned devices utilize dc conduction properties of Na^+-fast ionic conductors, another aim was to study the microstructural effects on the conduction properties of a whole glass-ceramic [23–27]. Special attention was paid to the analysis of grain boundary properties using the Na_2O–Y_2O_3–P_2O_5–SiO_2 system. For the analysis of grain boundary properties, as will be discussed below, composition dependences of the conductivity of sodium silico-phosphate glasses containing Y_2O_3 were also studied in the Na_2O–Y_2O_3–P_2O_5–SiO_2 system. For convenience, the present materials are abbreviated as NaRPSi taken from the initials of the Na_2O–R_2O_3–P_2O_5–SiO_2 system.

2 Materials

2.1 Preparation of glasses and glass-ceramics

Precursor glasses were prepared from reagent-grade oxides of anhydrous Na_2CO_3, R_2O_3 (R=Y, Sc, In, Er, Gd, Sm, Eu, Nd, La), $NH_4H_2PO_4$ and SiO_2; the mechanically mixed powders according to formula 2 or appropriate compositions shown below were melted at 1350 °C for 1 h after calcinations at 900 °C for 1 h. The melts were quickly poured into a cylindrical graphite, then annealed at 500 °C for 3 h, giving NaRPSi glasses. The composition parameters studied were in the range of $0.2<x<0.6$ and $0<y<0.5$ of formula 2. As shown below, grain boundary conduction properties are discussed in relation to the properties of glasses. For the evaluation of the composition dependence of conductivity in Na^+ conducting glasses, various sodium yttrium silico-phosphate glass specimens with different atomic ratios of [Na]/[P+Si] and [Na]/[Y] were also prepared.

Crystallization was carried out according to the previous report [13]; bulk glasses were heated with an increasing rate

of 75 °C/h to a temperature above approximately 50 °C of the glass transition point, which had been determined in advance by differential thermal analysis (DTA). This pretreatment was done in order to obtain homogeneous nucleation [22]. After the annealing for 1 h, specimens were heated at temperatures of 800 to 1100 °C, depending on the composition, for 0.5 to 72 h, thereafter slowly cooled in a furnace with a decreasing rate of 150 °C/h to room temperature. These quenched glasses or glass-ceramic specimens were polished down with 0.5 μm diamond paste, thereafter subjected to the conductivity measurements.

2.2 Measurements and characterization

Ionic conductivities were measured by the complex impedance method on cylindrical glasses or glass-ceramics of typically 15 mm in diameter and 2 mm in thickness. Electrodes were prepared by sputtering of gold on polished surfaces. The applied ac field ranged from 5 to 10 MHz in frequency. The temperature dependence of the conductivity was measured in a similar way at several temperatures ranging from room temperature to 350 °C. The complex impedance or admittance loci of glass and glass-ceramics were analyzed by an equivalent circuit (Fig. 2), which was experimentally found to comprise one and two semicircles in NaRPSi glasses and glass-ceramics, respectively. The two intercepting points on the real axis are interpreted as the resistance of crystallized grains ($R_{G(c)}$) and the total resistance of grains and remaining grassy grain boundaries ($R_{GB(g)}$). Assume the complex admittance diagram shown in Fig. 3, where the parameters L_1 and L_2 are set here as the radii of the two arcs 1 and 2. Those parameters are related to one another as the following:

$$L_1 \propto 1/\left(R_{G(c)}+R_{GB(g)}\right) \tag{4}$$

and

$$L_2 \propto \left(1/R_{G(c)}\right) - 1/\left(R_{G(c)}+R_{GB(g)}\right) \tag{5}$$

Then,

$$L_2/L_1 = R_{GB(g)}/R_{G(c)} \tag{6}$$

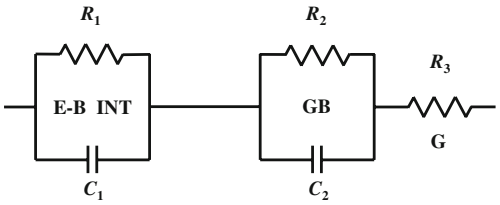

Fig. 2 Equivalent circuit employed for the admittance analysis. E-B INT, GB, and G represent the electrode-bulk interface, grain-boundaries and grains, respectively, and (R_1, C_1), (R_2, C_2), and R_3 are their resistances and capacitances

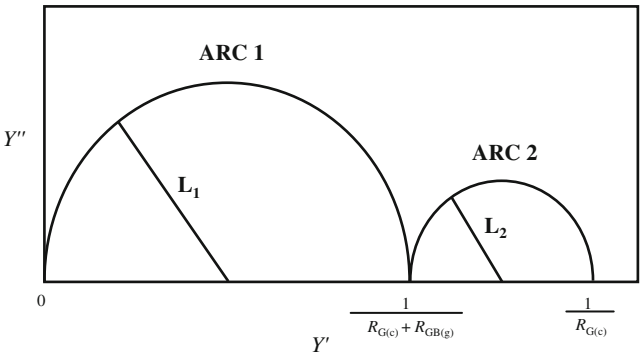

Fig. 3 An idealized diagram of complex admittance for glass-ceramics, in which arc 1 (ARC 1) and arc 2 (ARC 2) are related to the crystallized grains [G(c)] and remaining glasses [GB(g)]. L_1, L_2, $R_{G(c)}$, and $R_{GB(g)}$ are, respectively, the radii of arcs 1 and 2, the resistances of G(c) and GB(g)

Therefore, in an ideal grass-ceramic where residual grass would have negligible influence on the total, arc 2 would be much smaller than arc 1, since $L_2/L_1 \rightarrow 0$.

Crystalline phases of glass-ceramic specimens were identified by X-ray diffraction (XRD) method. The lattice parameters of the N5-type hexagonal unit cell were calculated by a least-squares method using the XRD peaks of (054), (044), (134), (440) and (024). Glass-ceramics of Y^{3+}-contained NaRPSi were subjected to scanning (SEM) and transmission electron microscope (TEM) for micro-structural analysis. Electron diffraction and compositional analyses were also performed to characterize the structure of the grain boundary.

For the description of a specific NaRPSi, R of the term will be replaced, respectively, with Y, Sc, In, Er, Gd, Sm, Eu, Nd and La as NaYPSi, NaScPSi, NaInPSi, NaErPSi, NaGdPSi, NaSmPSi, NaEuPSi, NaNdPSi and NaLaPSi for Y_2O_3, Sc_2O_3, In_2O_3, Er_2O_3, Gd_2O_3, Sm_2O_3., Eu_2O_3, Nd_2O_3 and La_2O_3.

3 Thermodynamic and kinetic study on the phase transformation

3.1 Composition dependence of precursor and high temperature stable phases

Figure 4 shows the composition dependence of both the precursor phases and the high temperature stable phases of glass-ceramic NaYPSi on the maps of phosphorus–yttrium [P–Y, Fig. 4(a)], yttrium–sodium [Y–Na, Fig. 4(b)] and phosphorus–sodium [P–Na, Fig. 4(c)], where the variables on the abscissas and ordinals are expressed with the composition parameters $1-x$, y and $3+3x-y$ for yttrium, phosphorus and sodium, respectively. As reported before [9, 20], N3- and N9-type NaYPSi glass-ceramics can be

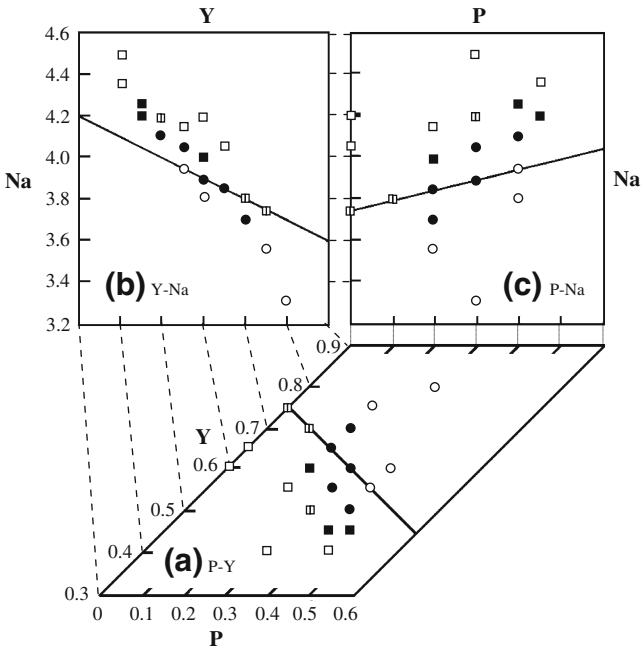

Fig. 4 Composition dependence of precursor (*pp*) and high temperature-stable phases (*sp*) of glass-ceramic NaRPSi on P–Y (**a**), Y–Na (**b**) and P–Na (**c**) maps, where precursor phases N3 and N9 are shown with *circles* and *squares*, respectively. High temperature-stable phases are shown in such a way that solid marks means that N5–NaRSi is the stable, while *open marks* indicate that the precursor phases are also stable even at high temperatures. Mixed phases are also shown: *open circle* pp = sp = N3; *filled circle* pp = N3, sp = N5; *open square* pp = sp = N9; *filled square* pp = N9, sp = N5; *open split square* pp = N9, sp = N9 + N5

crystallized as the high-temperature stable phases at the regions of higher [Y] ($1-x$>approximately 0.8) and rather lower [Y] ($1-x$<approximately 0.55), respectively, in the [Y]–[P] relation.

Concerning the precursor phases, only either N3- or N9-type NaYPSi was found in any composition, while N5-type NaYPSi was difficult to crystallize from glasses at low temperatures. It is also seen in the [P]–[Y] map [Fig. 4(a)] that, under a given phosphorus content ([P]<0.6) a composition with higher content of yttrium gives N3-type NaYPSi (open circle) as the precursor phase, while lower [Y] content results in N9-type phase (open square). The values of [Y] dividing the regions allowed for N3- and N9-type NaYPSi glass-ceramics decreased with increasing [P], and the boundary seems to locate slightly apart from the deduced line of [Y]=0.75−0.5[P] [9] shown with the solid line. Around the boundary region N5-type NaYPSi can be obtained as the stable phase at high temperatures (solid marks of circle or square). In the [Y]–[Na] or [P]–[Na] relations [Fig. 4(b) and (c)], the region where N5-type NaYPSi can be found as the high-temperature stable phase is found under approximately 3.6<[Na]<4.3. The effect of sodium content seems insignificant, because the value of [Na] is subordinately determined as [Na]=6−3[Y]–[P] (=3+3$x-y$) depending on the contents of both yttrium and phosphorus.

The above results may suggest that the [P]–[Y] relation dominates the region which is allowed for each NaYPSi at high temperatures. Considering this inference, we calculated the products of [P]×[Y] for all of the specimens. The values of [P]×[Y] were as follows (shown in Fig. 5); 0.16–0.25 for single phase N3-type NaYPSi, 0.14 for mixed phases of N3- and N5-type NaYPSi, 0.12–0.20 for single phase N5-type NaYPSi, 0–0.14 for the mixed phases of N5- and N9-type NaYPSi, and 0–0.17 for single phase N9-type NaYPSi, respectively. It was therefore deduced (Fig. 5) that the free energy of formation (ΔG_f) of N9-type NaYPSi would be the lowest in a lower region of [P]×[Y], N5-type NaYPSi may have the lowest ΔG_f in a medium [P]×[Y] region, and higher [P]×[Y] would lower ΔG_f of N3-type NaYPSi.

For a specimen in which N5-type NaYPSi is the stable phase at high temperatures, the aspect such as Fig. 6(a) would be illustrated in that ΔG of N3- or N9-type NaYPSi would be much smaller than that of N5-type NaYPSi near the crystallization temperature (T_c), and the value of N5-type NaYPSi would be lowered much less than of the two. Figure 6(b) indicates the aspect that ΔG or N3- or N9-type NaYPSi stable.

3.2 Kinetic effects of composition on the phase transformation

The kinetic effects of composition on the phase transformation are shown in Fig. 7, which compares the phase transformation rates of specimens $Na_{3.9}Y_{0.6}P_{0.3}Si_{2.7}O_9$ and $Na_{3.75}Y_{0.65}P_{0.3}Si_{2.7}O_9$. The transformation rate (α_v) of a

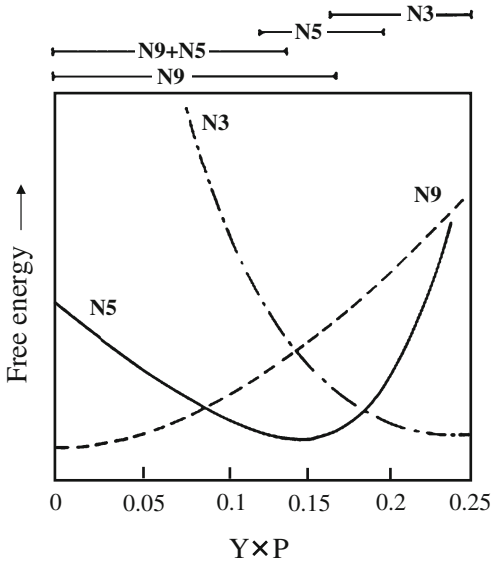

Fig. 5 Schematic figure of composition ([Y]×[P]) dependence of free energy of N5-, N3- and N9-type NaYPSi

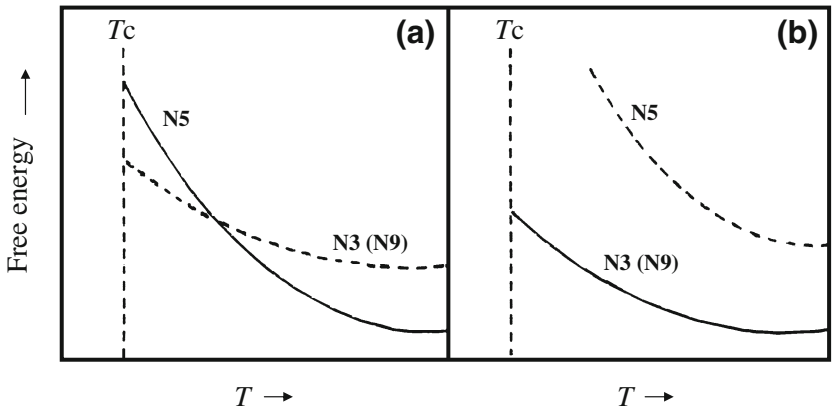

Fig. 6 Schematic figures of temperature dependence of free energy change of N5- and N3- or N9- type NaYPSi in the cases assuming N5- (**a**) and N3- (**b**) or N9-type (**b**) NaYPSi as the high temperature-stable phase, where *Tc* is the crystallization temperature

precursor phase to the stable N5 phase was determined as the weight ratio of N5-type NaYPSi in a glass-ceramic specimen. The value of α_v was experimentally obtained from the relationship of weight ratio to XRD intensity ratio, which relationship had been made previously by XRD intensity measurement on specimens with given weight ratio of N5-type NaYPSi to metastable phases. It is seen that the composition $Na_{3.9}Y_{0.6}P_{0.3}Si_{2.7}O_9$ is superior to the other, for the N5 single phase NaYPSi was difficult to obtain in the latter specimen. In specimen $Na_{3.9}Y_{0.6}P_{0.3}Si_{2.7}O_9$ a glass-ceramic of N5 single phase NaYPSi was easily obtained at a temperature higher than 900 °C for only three hours. The composition $Na_{3.75}Y_{0.75}Si_3O_9$ (or $Na_5YSi_4O_{12}$) was inferior in the same meaning.

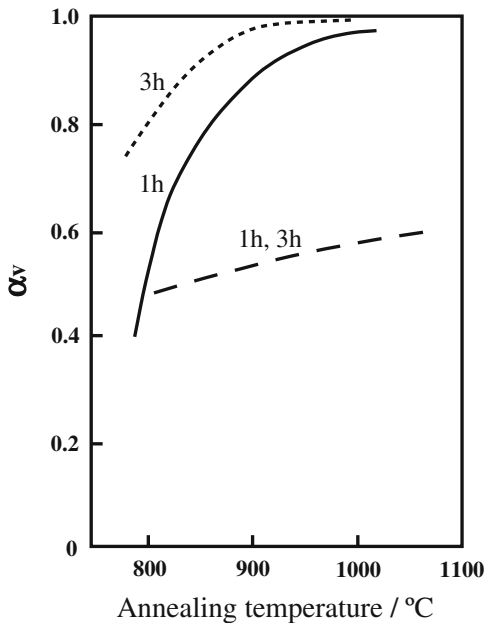

Fig. 7 Comparison of phase transformation rate (α_v) between specimens $Na_{3.9}Y_{0.6}P_{0.3}Si_{2.7}O_9$ (1-h annealing, *solid line*; 3-h annealing, *dotted line*) and $Na_{3.75}Y_{0.65}P_{0.3}Si_{2.7}O_9$ (1-h, 3-h-annealing, *dashed line*)

Figure 8 shows the kinetic characteristics of phase transformation of the metastable phase of N3- to N5-type NaYPSi of specimen $Na_{3.9}Y_{0.6}P_{0.3}Si_{2.7}O_9$ at various temperatures. The transition rates, α_v, of the silicophosphate NaYPSi were much higher than those of the $Na_{3.75}Y_{0.75}Si_3O_9$ silicate material.

The results shown were analyzed with the Avrami empirical equation, $\alpha_v = 1 - \exp(-kt^n)$, where k is the rate constant, and n is a constant. The data on α_v obtained at the initial and intermediate stages gave a linear relationship between $\ln(\ln(1-\alpha_v)^{-1})$ and $\ln(t)$ with a correlation coefficient of more than 0.99. The Avrami parameter and rate constants obtained are summarized in Table 1. Based on the Arrhenius relationship (Fig. 9), $k = A\exp(-E_v/RT)$ with E_v as the activation energy and constants A and R, on those k values which increased with increasing temperature, we obtained an activation energy of 1.2×10^3 kJ/mol, suggesting that the phase transformation can be rather difficult to take place. An addition of phosphorus and the excess sodium seem effective to the promotion of the phase transformation.

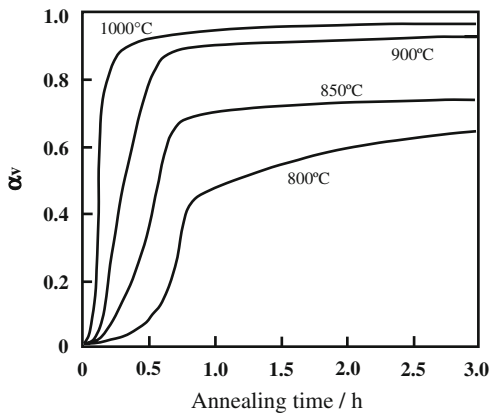

Fig. 8 Phase transformation rate (α_v) of N3- to N5-type NaYPSi on the specimen $Na_{3.9}Y_{0.6}P_{0.3}Si_{2.7}O_9$

Table 1 Kinetic parameters of phase-transformation of N3- to N5-type NaYPSi of $Na_{3.9}R_{0.6}Si_{2.7}O_9$.

Annealing temperature (K)	Avrami modulus n	In k
1073	2.61	−20.7
1123	1.94	−14.6
1173	1.39	−9.54
1223	0.75	−4.41

4 Microstructural effects on conduction properties

4.1 Crystallization and phase diagram

As expected from the previously reported results on NaYPSi [8], the crystallization of the fast ionic conducting N5-type phase took place, depending both on the contents of [R] and [P], at temperatures of 800 °C to 1000 °C in most NaRPSi glasses of Er to Sm except for scandium and lanthanum NaRPSi glasses. The N5 single phase region was wider for NaRPSi of smaller R, but was limited at the [P]≈0 region. The effect of phosphorus substitution for Si is important in the crystallization of N5-type phase. The composition 7

$$Na_{3.9}R_{0.6}P_{0.3}Si_{2.7}O_9 \quad (7)$$

was experimentally shown as the most appropriate composition for the crystallization of N5-type phase.

The relationship between the ionic radius of R^{3+} (r_R) and the hexagonal lattice parameters of N5-type single phase is consistent with the previous report [4] on $Na_5RSi_4O_{12}$ (R=Sc−Sm) in the tendency that both lattice parameters increased with increasing r_R. The elongation of these lattice axes is attributed to the octahedral coordination of R^{3+} with the O^{2-} of SiO_4- or PO_4-tetrahedra of the 12-membered rings. The local structure around R^{3+} ions is to be further discussed below in relation to conduction properties. On the formation of N5-type single phase, the incorporation of excess sodium ions [$4(3+3x-y)/3-5=(12x-4y-3)/3$ in composition 3] and substitution of rare earth ions [$1-4(1-x)/3=(4x-1)/3$] must be accounted for in view of N5-type crystal structure.

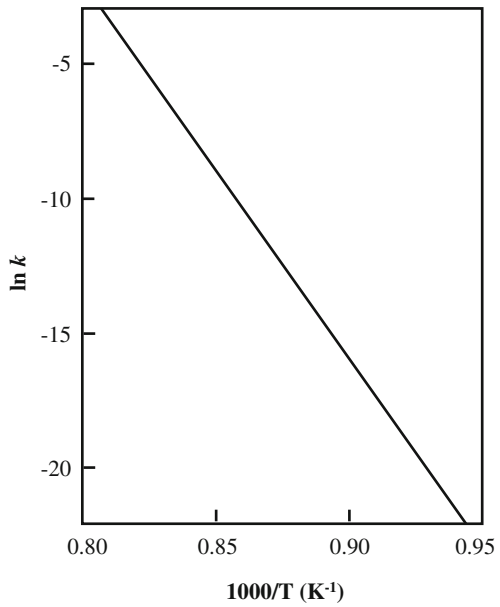

Fig. 9 Arrhenius-type plot of ln k with 1000/T of specimen $Na_{3.9}Y_{0.6}Si_{2.7}O_9$

Banks et al. [7] have reported the values of σ_{300} as 5×10^{-3} to 1×10^{-2} S/cm for glass-ceramic $Na_5RSi_4O_{12}$ (R=Er, Y, Gd, Sm), which are as low as those of the mixed phase NaRPSi specimens. The single phase N5-type glass-ceramic was not obtained in the present work. Based on the above crystallization analysis, their glass-ceramic specimens are reasonably considered to suffer from phase inhomogeneity brought about by insufficient annealing. The formation of N5-type structure from the precursor glasses is a matter of crystallization kinetics, since single-phase N5 has been synthesized in single crystal [2, 3, 28] or polycrystalline [5, 6, 10] form based on the composition of N5. It is noted here that the precursor phases identified were N3- or N9-type. Both N3 and N9 are considered to form iso-structural [11, 20, 29] with $Ca_3Al_2O_6$ [30] to be comprised of the skeleton structure of 6-membered SiO_4-tetrahedra rings [13]. It is generally known that phosphorus pentoxide acts as nucleating agent in the formation of glass-ceramics. It is therefore presumed at present that the substitution of an asymmetric PO_4-tetrahedron has the weakening effect on the bonding of the skeleton structure of 6-membered SiO_4-tetrahedra rings, resulting in the tendency to form the stable 12-membered structure.

4.2 Conduction properties of crystalline grains

The complex impedances and admittances of the measured NaRPSi glass-ceramics consisted of two semicircles below 300 °C. The two intercepting points on the real axis are interpreted as the resistance of crystallized grains (R_G) and the total resistance of grains and remaining glassy grain boundaries (R_{GB}). Shown in Fig. 10 are examples of the temperature dependence Arrhenius plots made on the basis of the calculated conductivity values of grains and grain boundaries of the glass-ceramic NaYPSi ($Na_{3.9}Y_{0.6}P_{0.3}Si_{2.7}O_9$) and NaSmPSi ($Na_{3.9}Sm_{0.6}P_{0.3}Si_{2.7}O_9$), in which the geometrical ratios of thickness to surface area for grains were also used for convenience for those of grain boundaries because of their undefinable shapes. Table 2 summarizes the measured conductivities (σ_{300}) and the calculated activation energies (E_a) assigned for grains of the glass-ceramics with composition 7 of Sc to La, regardless

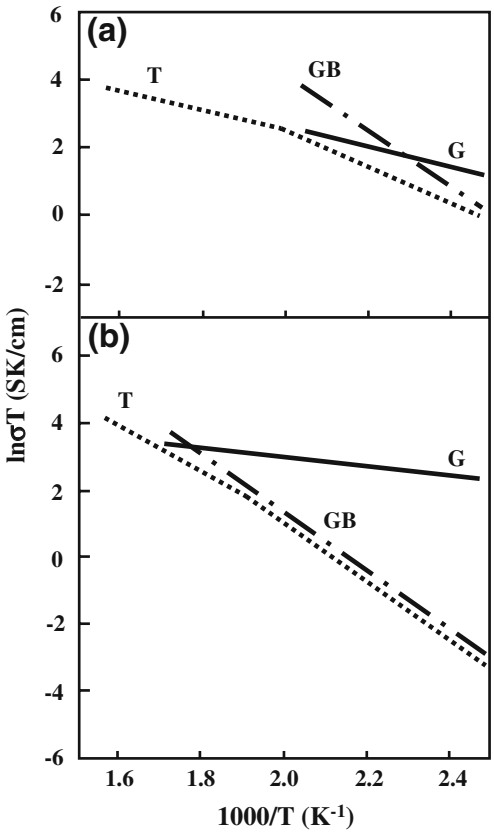

Fig. 10 The Arrhenius plots of the conductivities of grains (*G*), grain boundaries (*GB*) and the total bulk (*T*) of the glass-ceramic $Na_{3.9}Y_{0.6}P_{0.3}Si_{2.7}O_9$ (**a**) and $Na_{3.9}P_{0.3}Sm_{0.6}Si_{2.7}O_9$ (**b**)

of whether their crystalline phases are N5-type or not. The conductivities, σ_{300}, of single-phase NaRPSi specimens of Er to Sc range from 4×10^{-2} to 1×10^{-1} S/cm; in accordance the E_a falls in the range of 23 to 27 kJ/mol. In contrast, the mixed phase NaRPSi of Sc and In showed much smaller σ_{300} of 3×10^{-3} with an E_a of 35 to 40 kJ/mol, while non-NaRPSi glass-ceramics with unknown or mixed phases showed much lower conductivities of 1×10^{-5} to 1×10^{-4} S/cm with an E_a of 55 to 58 kJ/mol.

Table 2 Conduction properties of various NaRPSi glass-ceramics with composition $Na_{3.9}R_{0.6}Si_{2.7}O_9$.

R^{3+} (ions)	E_a kJ/mol	Conductivity (σ_{300})	Crystalline phase
Sc	35.3	3.2×10^{-3}	N5-type + unknown
In	39.8	3.1×10^{-3}	N5-type + unknown
Er	26.9	3.6×10^{-2}	N5-type
Y	26.6	6.6×10^{-2}	N5-type
Gd	23.0	1.3×10^{-1}	N5-type
Eu	24.4	5.2×10^{-2}	N5-type
Sm	20.9	6.3×10^{-2}	N5-type
Nd	55.1	2.2×10^{-5}	Unknown
La	57.8	1.6×10^{-4}	Unknown

The tendency of the conduction properties in single-phase NaRPSi specimens is consistent with the reported result measured on the corresponding polycrystalline $Na_5RSi_4O_{12}$ [4]; σ increased with increasing r_R. The previous works have proposed a mechanism that rare earth ions, octahedrally coordinated with the non-bridging oxide ions of the 12-membered rings of silica tetrahedra, work to expand the conduction paths for Na^+ ions along the *c*-axis [4, 28], which can explain the observed dependence of E_a on r_R in this work.

4.3 Structure and conduction properties of grain boundaries

As R_{GB} decreases rapidly with increasing temperature because of high $(E_a)_{GB}$ to a comparable value with R_G at 300 °C (Fig. 10), the total conductivities (R_G+R_{GB}) are dominated by grain boundary conductivity. The grain size-dependence of σ_{300} is therefore explained by the decrease in the number of poorly conductive grain boundaries with increasing grain size.

The conduction properties of grain boundaries were strongly dependent on the annealing conditions, although those of the grains were little changed by annealing temperature and time. Glass-ceramics are generally composites consisting of crystallized grains and small amounts of residual glass (<1%) [22]. To compare the properties of grain boundaries with those of glasses, the conduction properties of sodium yttrium silicophosphate glasses with various compositions were measured. Unlike glass-ceramics the impedance loci of glasses were comprised of one arc, which indicates that there is no polarization arising from microstructural inhomogeneity. Based on the intercepting points on the horizontal axis, the composition dependence of conduction properties of σ_{300} and E_a were evaluated. The value of σ_{300} ranged from 1×10^{-4} to 5×10^{-3} S/cm and E_a increased from 53 to 67 kJ/mol with [Na] or [Na]/[Y]. These results are also in good agreement with those reported for the glasses in the Na_2O–Y_2O_3–SiO_2 system [31]. The values of $(E_a)_{GB}$ of the specimens annealed below 950 °C for shorter times correspond to those in the range of glasses, strongly suggesting that their grain boundaries are a glassy matrix. The above mentioned dependence of $(E_a)_{GB}$ on [Na_2O] is explained by the well-known tendency that the conduction properties of glasses are improved by increasing [Na_2O], which provides the increase of carrier Na^+ ions. The ratio of [Na]/[Y] is also an important parameter for the conduction properties [31], showing an effect on the conduction properties similar to [Na_2O].

In order to identify the structure of the grain boundaries of the specimen ($Na_{3.9}Y_{0.6}P_{0.3}Si_{2.7}O_9$) annealed at 800 °C for 0.5 h, TEM analysis was performed both on grains and grain boundaries. The results show clear electron diffraction on grains, while not on grain boundaries. This fact confirms

that the grain boundaries are amorphous. Compositional analyses were also performed, however, [Na] was difficult to determine because of the evaporation by electron ablation. It was also observed that the glassy phase was condensed at triple points enclosed by grains, and that neck growth among the grains was well developed. Thus, it is reasonable to consider that the grain boundaries annealed at lower temperatures are amorphous, while those annealed at higher temperatures for longer periods of time are poorly conductive crystalline compounds in the specimens.

5 Summary

Na^+-fast ionic conducting glass-ceramics were produced using the sodium rare earth silicophosphate composition of $Na_{3+3x-y}R_{1-x}P_ySi_{3-y}O_9$, in which the rare earth elements of Sc to Sm were applicable to *R*. The meaning of the composition formula can be signified in the thermodynamic and kinetic study of crystallization and phase transformation of metastable to stable phase in the production of N5-type glass-ceramics. It was demonstrated that the medium value of content product as [P]×[R] is important in the crystallization of N5 single phase. Conduction properties of these glass-ceramics were strongly dependent upon the crystallization conditions as well as compositions. Not only complex impedance analysis but also TEM observation confirmed that this dependence was attributed to the conduction properties of grain boundaries which were glasses condensed at triple points enclosed by grains.

References

1. S. Morimoto, J. Ceram. Soc. Jpn. **97**, 1097 (1989)
2. B.A. Maksimov, Y.A. Kharitonov, A.N.V. Belov, Sov. Phys. Dokl. **18**, 763 (1974)
3. B.A. Maksimov, I.V. Petrov, A. Rabenau, H. Schulz, Solid State Ion. **6**, 195 (1982)
4. R.D. Shannon, B.E. Taylor, T.E. Gier, H.Y. Chen, T. Berzins, Inorg. Chem. **17**, 958 (1978)
5. H.U. Beyeler, T. Himba, Solid State Commun. **27**, 641 (1978)
6. H.Y.-P. Hong, J.A. Kafalas, M. Bayard, Mater. Res. Bull. **13**, 757 (1978)
7. E. Banks, C.H. Kim, J. Electrochem. Soc. **132**, 2617 (1985)
8. K. Yamashita, M. Tanaka, T. Umegaki, Solid State Ion. **58**, 231 (1992)
9. K. Yamashita, T. Nojiri, T. Umegaki, T. Kanazawa, Solid State Ion. **35**, 299 (1989)
10. R.D. Shannon, T.E. Gier, C.M. Foris, J.A. Nelen, D.E. Appleman, Phys. Chem. Miner. **5**, 245 (1980)
11. F. Cervantes, L.J. Marr, F.P. Glasser, Ceram. Int. **7**, 43 (1981)
12. C.H. Kim, B. Qiu, E. Banks, J. Electrochem. Soc. **132**, 1340 (1985)
13. K. Yamashita, S. Ohkura, T. Umegaki, T. Kanazawa, Solid State Ion. **26**, 279 (1988)
14. T. Okura, M. Tanaka, G. Sudoh, Mater. Res. Soc. Symp. Proc. **453**, 611 (1997)
15. T. Okura, K. Yamashita, T. Umegaki, Phosphorus Res. Bull. **6**, 237 (1996)
16. T. Okura, M. Tanaka, H. Monma, K. Yamashita, G. Sudoh, J. Ceram. Soc. Jpn. **111**, 257 (2003)
17. K. Yamashita, T. Umegaki, M. Tanaka, T. Kakuta, T. Nojiri, J. Electrochem. Soc. **143**, 2180 (1996)
18. T. Okura, M. Tanaka, H. Kanzawa, G. Sudoh, Solid State Ion. **86-88**, 511 (1996)
19. K. Yamashita, M. Tanaka, T. Kakuta, M. Matsuda, T. Umegaki, J. Alloys Comp. **193**, 283 (1993)
20. K. Yamashita, T. Nojiri, T. Umegaki, T. Kanazawa, Solid State Ion. **40**(41), 48 (1990)
21. K. Yamashita, S. Ohkura, T. Umegaki, T. Kanazawa, J. Ceram. Soc. Jpn. **96**, 967 (1988)
22. W.D. Kingery, H.K. Bowen, D.R. Uhlmann, *Introduction to Ceramics*, 2nd edn. (Wiley, New York, 1976), p. 368
23. T. Okura, H. Monma, K. Yamashita, J. Ceram. Soc. Jpn. **112**, S685 (2004)
24. T. Okura, H. Monma, K. Yamashita, Solid State Ion. **172**, 561 (2004)
25. T. Okura, K. Yamashita, Solid State Ion. **136**(137), 1049 (2000)
26. T. Okura, Y. Inami, H. Monma, S. Nakamura, K. Yamashita, Solid State Ion. **154**, 361 (2002)
27. T. Okura, H. Monma, K. Yamashita, J. Eur. Ceram. Soc. **26**, 619 (2006)
28. H.U. Beyler, R.D. Shannon, Appl. Phys. Lett. **37**, 934 (1980)
29. I. Maki, T. Sugimura, J. Ceram. Soc. Jpn. **78**, 129 (1970)
30. P. Mondal, J.W. Jeffery, Acta Cryst. **B31**, 689 (1975)
31. M.G. Alexander, Solid State Ion. **22**, 257 (1987)